CZ9726834 P-2-90

Electron Beam Effects on the Spectroscopy of Satellite Lines in Aluminum X–Pinch Experiments

J. Abdallah, Jr.[1], A. Ya. Faenov[2], D. A. Hammer[3], S. A. Pikuz[4], G. Csanak[1], R. E. H. Clark[1], V. M. Romanova[4], and T. A. Shelkovenko[4]

[1]*Los Alamos National Laboratory, Los Alamos, New Mexico 87545*
[2]*MISDC, NPO "VNIIFTRI", Mendeleevo, Moscow region, 141570 Russia*
[3]*Cornell University, Ithaca, New York*
[4]*P. N. Lebedev Physical Institute, Moscow, Russia*

Abstract

Aluminum wire X–pinch experiments performed at the Cornell University XP pulsed power generator and at the Lebedev Institute BIN generator show detailed high resolution spectra for satellilte lines of Li–like, Be–like, B–like, and C–like ions. These lines, which correspond to transitions originating from autoionizing levels, are observed in the direction of the anode with respect to the bright X–pinch cross point. The intensities of these satellites are much smaller or absent in the direction of the cathode. Such transitions are caused by collisions of ions with energetic electrons (5–15 keV) which are created by the inductive voltage drop between the cross point and the anode. A collisional–radiative model was constructed using a non–Maxwellian electron energy distribution consisting of a thermal Maxwellian part plus a Gaussian part to represent the high energy electron beam. The shapes of the observed satellite structures are consistent with the calculated spectrum for electron temperatures between 30–100 eV, and beam densities of about 10^{-7} times the plasma electron density.

The purpose of the present work is to study in detail the spectroscopy of satellite lines which are observed in X-pinch produced plasmas. Satellite emission lines are observed from the Li-like, Be-like, B-like, and C-like ion stages of aluminum. The transitions correspond to the radiative $2p \rightarrow 1s$ decay of autoionizing levels having a $1s$ shell vacancy. The satellite lines are observed only toward the anode side of the x-pinch cross point. The upper levels are populated mainly by electron impact excitation and ionization of $1s$ shell electrons in relatively cold regions of plasma and by dielectronic recombination to a lesser extent. The high energy electrons which are required to stimulate such transitions are produced by the inductive voltage drop from the cross-point to the anode, in effect forming an electron beam. This explains why the satellite lines are much less intense or absent on the cathode side of the hot spot (see below). Dielectronic recombination due to thermal electrons is also important for determining the spectral line structures.

The experiments were performed using the XP pulser at Cornell University operating at about 350 kA peak current in a 100 ns pulse and the BIN generator at Lebedev Institute with a current of 250 kA in a 100 ns pulse.

High temperature and high density X-pinch plasmas were created during the explosion process which occurs when two or more crossed wires are placed between the output

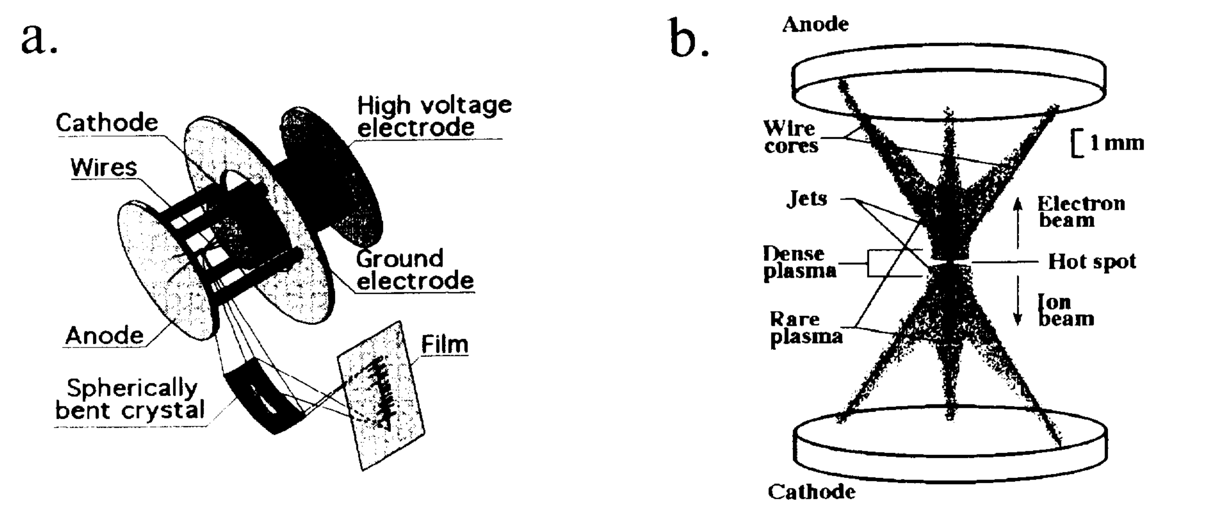

Figure 1: a) Schematic diagram of the X-pinch experiment including an x-ray spectrograph; b) Schematic diagram of the plasma regions formed in the X-pinch.

electrodes of the pulser diode (Fig. 1). The plasmas created were studied using various diagnostics in different spectral ranges. The spectra of highly charged ions in the x-ray region were obtained using the Focusing Spherical spectrograph with one dimensional Spatial Resolution (FSSR-1D)[1,2]. This spectrograph is constructed with mica crystals curved on a 100 mm spherical surface. The spatial resolution in these experiments was better than 50 microns. However, in principle, 10 microns can be achieved. The spectral resolution of the spectrograph $\lambda/\Delta\lambda$ exceeds 3000 and does not depend on the size of the plasma[3]. This is the most important feature for recording the radiation emitted by the diffuse plasma surrounding the x-pinch bright spot.

A spectrogram obtained with the XP-pulser using crossed aluminum wires is shown in Fig. 2. Note that the spectrum is resolved in one spatial dimension and integrated in time. Densitograms of this spectrum are shown on both sides of the wire cross point. The strong asymmetry of the line radiation relative to the cross point is obvious. The resonance and intercombination lines of He-like Al ions were recorded on both sides of the cross point in the second order of the mica crystal reflection. Strong satellite lines corresponding to transitions in Li-like through C-like aluminum were observed in the anode direction and were only weakly observed or absent in the cathode direction. Lines corresponding to $np \rightarrow 1s$ transitions in H-like Al ions were also observed (not shown) in the cathode direction. These lines were recorded in the third order of the mica crystal reflection. The presence of lines belonging to H-like aluminum make it possible to measure the wavelengths of satellite lines with an accuracy of 3–5 mA. The spectra were recorded on KODAK DEF film and the images were digitized using an OPTRONICS PHOTOSCAN densitometer with a 12.5 micron pixel size.

The population densities of the atomic levels were deduced from non-equilibrium steady-state kinetics calculations and were used as input for the spectral simulations. The rate coefficients, used in the evaluation of the rate equations, were computed with a non-equilibrium electron energy distribution. In general, the rate coefficient for a process involving a collision of a single electron with an ion in initial state i which induces a transitions to a final state j is given by[4]

$$r_{ij} = \int F(E)v(E)\sigma_{ij}dE, \qquad (1)$$

where E is the electron energy, $F(E)$ is the electron energy distribution function, v is the associated velocity $(2E/m)^{1/2}$, m is the electron mass, and σ_{ij} is the cross section. Eq.

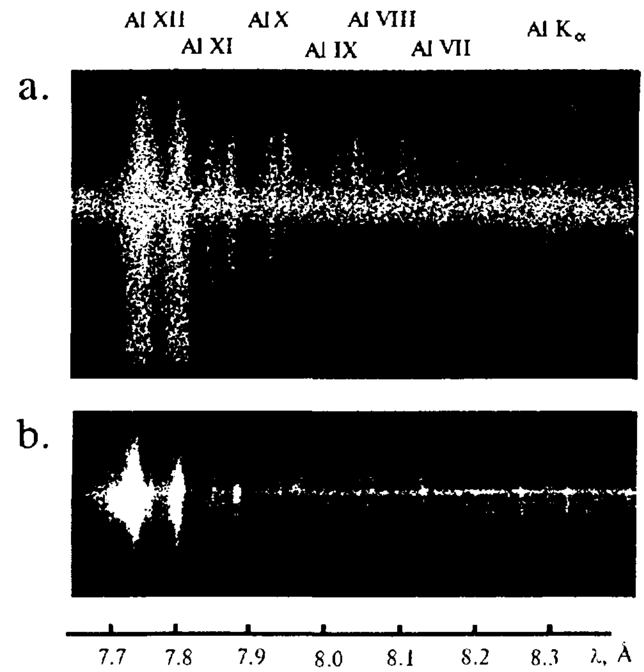

Figure 2: A FSSR-1D spectrum from an aluminum plasma produced by crossed wires in the XP-pulser (a) and in the BIN-generator (b).

1 corresponds to a weighted average of the cross section for a particular distribution of electron energy. All integrals presented in this section are evaluated on the interval $0 \leq E \leq \infty$. For an X-pinch plasma in the direction of the anode the effect of both thermal electrons and beam electrons must be incorporated into the electron energy distribution function. For the present application the function

$$F = (1 - f)F_0(E, T) + fG(E, E_0, \Gamma) \tag{2}$$

was chosen. In Eq. 2 f is the beam fraction, which is the fraction of the total free electron density involved in the beam, F_0 is the Maxwellian function which represents the thermal electrons, and G is the Gaussian function chosen to represent the beam electrons. The Maxwellian function is given by the usual relationship

$$F_0(E, T) = \frac{2}{\pi^{1/2}} \frac{E^{1/2} e^{-E/kT}}{(kT)^{3/2}}, \tag{3}$$

where kT corresponds to the temperature of the distribution in units of energy, and k is the Boltzmann constant. The Gaussian function is given by

$$G(E, E_0, \Gamma) = gE^{1/2} e^{-(E-E_0)^2/(2\Gamma^2)} \tag{4}$$

where E_0 is the center of the Gaussian, Γ is its width, and g is a normalization constant. The functions F, F_0, and G are normalized such that

$$\int F dE = \int F_0 dE = \int G dE = 1. \tag{5}$$

See Ref. 5 which uses a similar method for including the effects of high energy electrons.

A detailed fine structure atomic model for the He-like through C-like ionization stages of aluminum was calculated using the Los Alamos suite of atomic physics codes[6,7]. The full effects of intermediate coupling and configuration interaction were included. The level structure corresponding to the configurations $1s^2(2s2p)^w$, $1s^2(2s2p)^{w-1}3l$, $1s^1(2s2p)^{(w+1)}$, and $1s^1(2s2p)^w3l$ was calculated for the Li–like through C–like ion stages.

The spectra were constructed using Lorentz line shapes with widths approximating the experimental resolution. Since satellite lines are generally weak and optically thin, and the plasma density is low, optical depth effects have been neglected. Figure 3a shows a comparison of a calculated spectrum with $kT = 40$ eV and $f = 10^{-7}$ with the experiment in the spectral range appropriate for B–like satellite lines. The figure also includes the C–like contribution. Several features in the spectra are not accounted for by the simulations. Figure 3b shows comparison of experimental and calculated spectra for the Be–like stage of ionization. The calculated spectrum corresponds to a temperature of 60 eV and $f = 10^{-7}$. The calculated spectrum is in excellent agreement with experiment. Figure 3c is comparison of experimental and calculated spectra for the Li–like stage of ionization. The calculated spectrum corresponds to an electron temperature of 80 eV and $f = 3 \times 10^{-7}$. Note that there seems to be a slight inconsistency between the calculated wavelengths and the calibration of the experimental measurement. However, the overall agreement between theory and experiment is quite good. The study shows that these structures can be reproduced by calculations with electron beam fractions $f \sim 10^{-7}$, in agreement with experimental estimates. The calculations also suggest that a temperature gradient from approximately 30 to 80 eV is formed in the plasma.

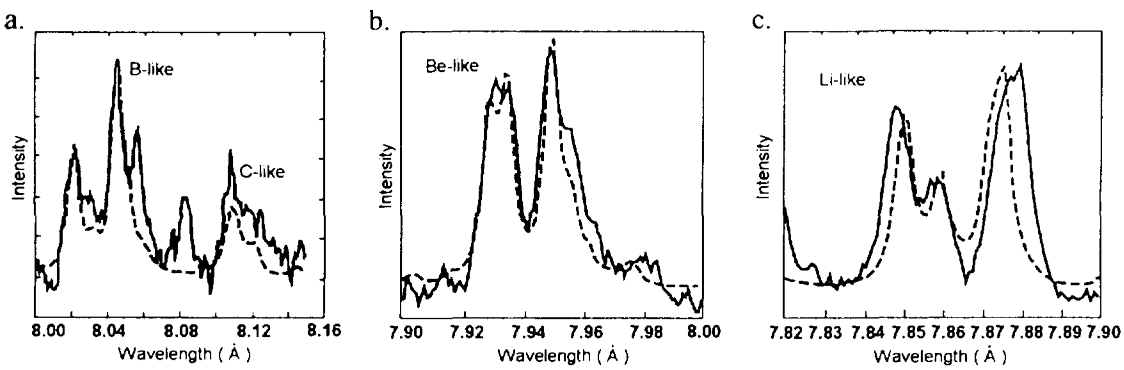

Figure 3: A comparison of the calculated spectrum (dashed line) with experiment (solid line).

References

[1] A.Ya. Faenov, Yu.A. Agafonov, B.A. Bryunetkin, V.M. Dyakin, A.I. Erko, G.V. Ivanenkov, A.R. Mingaleev, S.A. Pikuz, T.A. Pikuz, V.M. Romanova, and T.A. Shelkovenko, Proceedings of the International Society for Optical Engineering Meeting SPIE–93, San Diego CA, July 1993, 2015, p. 64.

[2] A.Ya. Faenov, Yu.A. Agafonov, S.A. Pikuz, A.I. Erko, B.A. Bryunetkin, V.M.Dyakin, G.V. Ivanenkov, A.R. Mingaleev, T.A. Pikuz, V.M. Romanova, and T.A. Shelkovenko, Physica Scripta 50, 333 (1994)

[3] V.A. Boiko, A.V. Vinogradov, S.A. Pikuz, I.Yu. Skobelev, and A.Ya. Faenov, Journal of Soviet Laser Research 6, 105 (1985)

[4] Ya.B. Zel'dovich and Yu.P. Raizer, Physics of Shock Waves and High Temperature Hydrodynamic Phenomena, Academic Press, New York and London (1966)

[5] F.B. Rosmej, JQSRT 51, 319 (1994)

[6] J. Abdallah, Jr. and R.E.H. Clark, Los Alamos National Laboratory reports, LA-11436-M, I-V (1988)

[7] J. Abdallah, Jr., R.E.H. Clark, J.M. Peek, and C.J. Fontes, JQSRT 51, 1 (1994)